

Theoretical considerations on factors confounding the interpretation of the oceanic carbon export ratio

Zuchuan Li^{1,2*}, Nicolas Cassar¹

¹ Division of Earth and Ocean Sciences, Nicholas School of the Environment, Duke University, Durham, North Carolina, USA

² Now at Woods Hole Oceanographic Institution, Woods Hole, Massachusetts, USA

* Corresponding author: Zuchuan Li (zuchuanli@whoi.edu)

Key points

1. Mechanistic models of the export ratio integrated over various depths are developed based on the metabolic balance between photosynthesis and respiration
2. Discrepancies between studies on the relationship between the export ratio and taxonomy, temperature and productivity, may be explained by a variety of factors, including the depths of integration, biomass, and surface light availability
3. Seasonal variability in the export ratio in high latitudes is in great part controlled by mixed layer depth and photosynthetically active radiation
4. Our study demonstrates and discusses some of the mathematical and biogeochemical limitations of the export ratio, arguing for improvements or the development of new proxies

This article has been accepted for publication and undergone full peer review but has not been through the copyediting, typesetting, pagination and proofreading process which may lead to differences between this version and the Version of Record. Please cite this article as doi: 10.1029/2018GB006003

Abstract

The fraction of primary production exported out of the surface ocean, known as the export ratio (*ef*-ratio), is often used to assess how various factors, including temperature, primary production, phytoplankton size and community structure, affect the export efficiency of an ecosystem. To investigate possible causes for reported discrepancies in the dominant factors influencing the export efficiency, we develop a metabolism-based mechanistic model of the *ef*-ratio. Consistent with earlier studies, we find based on theoretical considerations that the *ef*-ratio is a negative function of temperature. We show that the *ef*-ratio depends on the optical depth, defined as the physical depth times the light attenuation coefficient. As a result, varying light attenuation may confound the interpretation of *ef*-ratio when measured at a fixed depth (e.g., 100 m) or at the base of the mixed layer. Finally, we decompose the contribution of individual factors on the seasonality of the *ef*-ratio. Our results show that at high latitudes, the *ef*-ratio at the base of mixed layer is strongly influenced by mixed layer depth and surface irradiation on seasonal timescales. Future studies should report the *ef*-ratio at the base of euphotic layer, or account for the effect of varying light attenuation if measured at a different depth. Overall, our modeling study highlights the large number of factors confounding the interpretation of field observations of the *ef*-ratio.

Key words: Oceanic carbon export ratio, net community production, export production, net primary production

1. Introduction

The importance of relating oceanic carbon export to primary production has long been recognized. Building on *Dugdale and Goering* [1967] apportionment of primary production into “new” and regenerated production, *Eppley and Peterson* [1979] proposed to normalize new production to primary production (f -ratio). These seminal papers prompted complementary efforts to characterize the factors influencing the f -ratio, and the ratio of organic carbon export or particulate organic carbon (POC) export to total primary production (e-ratio and pe-ratio, respectively) [*Aksnes and Wassmann*, 1993; *Baines et al.*, 1994; *Betzer et al.*, 1984; *Dunne et al.*, 2005; *Henson et al.*, 2011; *Laws et al.*, 2000; *Michaels and Silver*, 1988; *Murray et al.*, 1996]. Whereas the f -ratio reflects the proportion of primary production fueled by “new” nutrients (or not fueled by regenerated nutrients), the e-ratio reflects the proportion of primary production exported (i.e., which has escaped respiratory processes). In a steady-state system with no change in elemental stoichiometry and no nitrification at the ocean surface, the f -ratio and e-ratio should be equal as export production should balance new production. Hereafter, we use the term “ ef -ratio” following *Laws et al.* [2000] to describe the ratio of new or export production.

Among other things, the ef -ratio has been hypothesized to vary as a function of sea surface temperature (SST), net primary production (NPP), respiration and sinking rates of particles. The negative relationship between the ef -ratio and SST reported in some studies has been attributed to the stronger temperature dependency of respiration compared to photosynthesis [*Cael and Follows*, 2016; *Dunne et al.*, 2005; *Henson et al.*, 2011; *Laws et al.*, 2000; *Laws et al.*, 2011; *Rivkin and Legendre*, 2001]. A positive relationship between the ef -ratio and NPP and/or phytoplankton biomass concentration has also been reported in various regions of the world oceans [*Dunne et al.*, 2005; *Eppley and Peterson*, 1979; *Huang et al.*, 2012; *Laws et al.*, 2011; *Laws et al.*, 2000]. Conversely, the sinking rate of particles is

expected to vary as a function of their density and size [Allredge and Silver, 1988], which are in turn related to the mineral content of the particles [Armstrong *et al.*, 2002; Francois *et al.*, 2002; Klaas and Archer, 2002], aggregation [Burd and Jackson, 2009; Passow *et al.*, 1994], and plankton community structure [Boyd and Newton, 1995; Boyd and Newton, 1999; Buesseler, 1998; Guidi *et al.*, 2016; Michaels and Silver, 1988]. These factors are often interconnected, which may explain the difficulty in identifying and quantifying the dominant factors. For example, some plankton types are generally associated with high production (NPP) and biomass regimes, which may also influence aggregation [Jackson and Kiorboe, 2008; Passow *et al.*, 1994].

In this vein, Britten *et al.* [2017] attributed to confounding factors the recent report of a lack of dependency of the carbon export efficiency on temperature in the Southern Ocean [Maiti *et al.*, 2013]. According to their “temperature-ballast” hypothesis, changes in ballasting masked the effect of temperature on the export efficiency [Britten *et al.*, 2017; Henson *et al.*, 2015]. An inverse relation of the export efficiency on NPP in the Southern Ocean as reported by Maiti *et al.* [2013] also prompted various hypotheses for mechanisms, including trophic structure, grazing and fecal pellet production, bacterial activity and recycling, and dissolved organic carbon (DOC) export [Cavan *et al.*, 2015; Laurenceau-Cornec *et al.*, 2015; Le Moigne *et al.*, 2016; Maiti *et al.*, 2013]. As importantly, a lack of steady-state, for example with export lagging production [Buesseler, 1998; Buesseler *et al.*, 2009; Henson *et al.*, 2015] would also bias estimates of the export ratio.

However, more fundamental factors, even at steady-state, may also explain the large scatter in the relation of the carbon export efficiency on predictors. For example, the depth of the measurements [Boyd *et al.*, 1995; Buesseler and Boyd, 2009; Palevsky and Doney, 2018], and the depth of the mixed layer in absolute terms and in relation to the depth of measurement of the *ef*-ratio may also introduce noise. As stated by Buesseler [1998], “since

both production and particulate export are strongly depth dependent, the relative ratio of these will depend upon the depth of integration.” The net production of organic matter, aka net community production (NCP) and which reflects the carbon export potential as presented in *Li and Cassar* [2017], is depth-dependent because it results from the balance between photosynthesis, which decreases with depth, and respiration. Conversely, POC export is depth-dependent because of remineralization and POC attenuation with depth. Such concepts are important but often overlooked when interpreting differences in ef -ratios between ecosystems and between studies.

In this study, we explore how some of these factors may confound the interpretation of the ef -ratio using a mechanistic model of the metabolic balance between photosynthesis and respiration. Using this model, we first compare ef -ratios at different depths of integration (i.e., euphotic depth (1% of surface irradiance), fixed depth, and mixed layer depth) and discuss factors regulating their relations to NPP. For example, two identical plankton communities may have diverging ef -ratios because of differences in mixed layer depth, with shallower mixed layers leading to higher ef -ratios. Similarly, our theoretical considerations predict that two ecosystems with differing autotrophic biomass and growth rates but equivalent NPP will display different ef -ratios, with the greater growth rates leading to a higher ef -ratio. Finally, we partition and examine the influence of the individual factors (i.e., mixed layer depth, surface irradiance, SST, nutrient concentration, and chlorophyll concentration) on the seasonality of the ef -ratio at the base of mixed layer of the world’s oceans.

2. Model description

By definition, the volumetric NCP at depth z ($NCP(z)$) is equal to the volumetric NPP ($NPP(z)$) minus the volumetric heterotrophic respiration ($HR(z)$) [*Li and Cassar*, 2017]:

$$\begin{aligned}
NCP(z) &= NPP(z) - HR(z) \\
&= N_m \times I_m(z) \times \mu_{max} \times C - r_{HR} \times C \quad (1)
\end{aligned}$$

where C , μ_{max} , N_m , $I_m(z)$, and r_{HR} represent the phytoplankton biomass concentration and maximum growth rate, the effects of nutrient concentration and light availability on the phytoplankton growth rate, and the heterotrophic respiration rate, respectively (see Table 1 for a list of acronyms and definitions). N_m , μ_{max} , r_{HR} , and C are assumed to be homogeneous above the depth of integration. Neglecting light inhibition, N_m and $I_m(z)$ can be modeled to obey Michaelis-Menten kinetics [Dutkiewicz *et al.*, 2001; Huisman and Weissing, 1994]:

$$N_m = \frac{N}{N + k_m^N} \quad (2)$$

$$I_m(z) = \frac{I(z)}{I(z) + k_m^I} \quad (3)$$

where N and k_m^N represent the nutrient concentration and half-saturation constant, respectively; and I and k_m^I stand for the photosynthetically active radiation (PAR) level and half-saturation constant, respectively. PAR at depth z ($I(z)$) exponentially decays with depth according to the following equation:

$$I(z) = I_0 \times e^{-K_I \times z} \quad (4)$$

where I_0 and K_I represent PAR just beneath the water surface, and the light attenuation coefficient, respectively. In the open ocean, K_I is modeled as an empirical function of the light attenuation coefficient at the wavelength of 490 nm ($K_d(490)$), which is in turn derived from the chlorophyll a concentration ($[Chl]$) [Morel *et al.*, 2007]:

$$K_I = 0.0665 + 0.874 \times K_d(490) - \frac{0.00121}{K_d(490)} \quad (5a)$$

$$K_d(490) = 0.0166 + 0.0773 \times [Chl]^{0.6715} \quad (5b)$$

where the constant '0.0166' is the light attenuation at 490 nm due to pure seawater; and the second term on the right-hand side of equation (5b) represents the light attenuation

coefficient due to non-water components (e.g., phytoplankton and colored dissolved organic matter). K_I and $K_d(490)$ increase with $[Chl]$ ($\frac{dK_d(490)}{d[Chl]} > 0$, and $\frac{dK_I}{d[Chl]} > 0$).

3. Influence of the depth of measurements on the export production and export ratio

In order to evaluate how the depth of integration influences export production and the ef -ratio, we derive equations describing these properties at the base of the euphotic layer and at a fixed depth (Table 2). To that end, we use equations (1-5) and build on the model presented in *Li and Cassar* [2017]. For simplicity, we assume that μ_{max} , r_{HR} , N , k_m^N , k_m^I , $[Chl]$, and C in equations (1-5) are well mixed or constant within the depth of integration. We also assume that the ecosystem is at steady state, and thus that export production is equal to NCP and new production.

3.1. Export ratio at the base of euphotic layer

Based on equation (1), NCP integrated over the euphotic layer ($NCP(0, Z_{eu})$) may be expressed as follows [*Li and Cassar*, 2017]:

$$\begin{aligned} NCP(0, Z_{eu}) &= NPP(0, Z_{eu}) - HR(0, Z_{eu}) \\ &= \int_0^{Z_{eu}} NPP(z) dz - \int_0^{Z_{eu}} HR(z) dz \\ &= N_m \times I_m(0, Z_{eu}) \times \mu_{max} \times C - r_{HR} \times C \times Z_{eu} \end{aligned} \quad (6)$$

where $NPP(0, Z_{eu})$ and $HR(0, Z_{eu})$ represent NPP and HR integrated over the euphotic zone, respectively; Z_{eu} denotes the euphotic depth where 1% of surface PAR remains; and $I_m(0, Z_{eu})$ is calculated from equations (3-4) as follows:

$$I_m(0, Z_{eu}) = \int_0^{Z_{eu}} I_m(z) dz = -\frac{1}{K_I} \times \ln\left(\frac{I_0 \times e^{-K_I \times Z_{eu}} + k_m^I}{I_0 + k_m^I}\right) \quad (7)$$

where

$$Z_{eu} = -\frac{\ln(0.01)}{K_I} \quad (8)$$

The autotrophic carbon to $[Chl]$ ratio ($C: [Chl]$) influences how $NCP(0, Z_{eu})$, $NPP(0, Z_{eu})$, and $HR(0, Z_{eu})$ respond to changes in C (Figure 1 and supplementary material). Intuitively, one would expect $NCP(0, Z_{eu})$, $NPP(0, Z_{eu})$, and $HR(0, Z_{eu})$ to monotonically increase with C , which is observed when $C: [Chl]$ ratio is a constant. However, when accounting for the varying $C: [Chl]$ ratio, $NCP(0, Z_{eu})$, $NPP(0, Z_{eu})$, and $HR(0, Z_{eu})$ plateau at high C .

This can be explained by: (1) the shoaling depth of integration Z_{eu} resulting from decreasing light availability with increasing C and $[Chl]$ (equations 5 and 8); and (2) the balance between phytoplankton physiology ($C: [Chl]$) and the package effect on light attenuation (equation 5b). It is worth noting that the responses of euphotic-depth integrated NCP, NPP and HR to variations in C are markedly different from the ones presented in Figure 2 of *Li and Cassar* [2017], where the rates were integrated to a fixed depth (e.g., mixed layer depth) as opposed to the euphotic depth.

The export ratio at the base of euphotic zone (ef_{eu}) can be derived from equation (6):

$$ef_{eu} = \frac{NCP(0, Z_{eu})}{NPP(0, Z_{eu})} = 1 - \frac{1}{\bar{I}_{eu}} \times \frac{1}{N_m} \times \frac{r_{HR}}{\mu_{max}} \quad (9)$$

where $\bar{I}_{eu} = \frac{I_m(0, Z_{eu})}{Z_{eu}} = \frac{1}{Z_{eu}} \times \int_0^{Z_{eu}} I_m(z) dz$ represents the averaged effect of light availability

on the phytoplankton growth rate in the euphotic zone which is independent of $[Chl]$

(equations 7-8). The right-hand side of equation (9) shows that ef_{eu} is a function of the

proportion of NPP not respired within the euphotic zone ($ef_{eu} = 1 - \frac{HR(0, Z_{eu})}{NPP(0, Z_{eu})}$). μ_{max} and

r_{HR} can be modeled to vary as a function of temperature (T) according to the following

equations [*Eppley*, 1972; *Lopez-Urrutia et al.*, 2006; *Rivkin and Legendre*, 2001]:

$$\mu_{max} \propto e^{P_t \times T} \quad (10)$$

$$r_{HR} \propto e^{B_t \times T} \quad (11)$$

and therefore:

$$\frac{r_{HR}}{\mu_{max}} = \beta \times e^{(B_t - P_t) \times T} \quad (12)$$

where P_t and B_t represent constants; and β is a parameter related to the community structure [Lopez-Urrutia *et al.*, 2006]. See Table 1 for the values attributed to these parameters.

3.2. Export ratio at a fixed depth

To investigate how export production and the ef -ratio at a fixed depth Z_z (ef_z) varies with Z_{eu} and $[Chl]$, we consider the two cases when the measurement depth is deeper and shallower than the euphotic depth ($Z_z > Z_{eu}$ and $Z_z < Z_{eu}$, respectively).

3.2.1. Measurement depth deeper than the euphotic depth

Assuming that particle flux below Z_{eu} exponentially decays with depth [Armstrong *et al.*, 2002; Lutz *et al.*, 2002], export production (F) when $Z_z > Z_{eu}$ can be estimated as follows:

$$F(Z_z) = F(Z_{eu}) \times e^{-\frac{Z_z - Z_{eu}}{Z^*}} \quad (13)$$

where Z^* is the remineralization length scale; and $F(Z_{eu})$ is equal to $NCP(0, Z_{eu})$ at steady state. Equation (9) and equation (13) lead to ef_z :

$$ef_z = \frac{NCP(0, Z_{eu})}{NPP(0, Z_{eu})} \times e^{-\frac{Z_z - Z_{eu}}{Z^*}} = ef_{eu} \times e^{-\frac{Z_z - Z_{eu}}{Z^*}} \quad (14)$$

Equation (14) suggests that ef_z is smaller than ef_{eu} and increases with deepening Z_{eu} because of lower particle flux attenuation (Figure 2(A)). Since Z_{eu} shoals with increasing $[Chl]$, ef_z is expected to be negatively related to $[Chl]$. As the depth of measurement deepens (i.e., increase Z_z), ef_z decreases because of the increasing contribution of remineralization processes. The general form of the relation between ef_z and Z_{eu} does not change if the particle attenuation in equation (14) is modeled using the Martin curve [Martin *et al.*, 1987].

3.2.2. Measurement depth shallower than the euphotic depth

When $Z_z < Z_{eu}$, export production and ef at Z_z may be expressed as follows:

$$\begin{aligned}
NCP(0, Z_z) &= NPP(0, Z_z) - HR(0, Z_z) \\
&= \int_0^{Z_z} NPP(z) dz - \int_0^{Z_z} HR(z) dz \\
&= N_m \times I_m(0, Z_z) \times \mu_{max} \times C - r_{HR} \times C \times Z_z \quad (15)
\end{aligned}$$

$$ef_z = \frac{NCP(0, Z_z)}{NPP(0, Z_z)} = 1 - \frac{1}{\bar{I}_z} \times \frac{1}{N_m} \times \frac{r_{HR}}{\mu_{max}} \quad (16a)$$

$$ef_z = \frac{NCP(0, Z_z)}{NPP(0, Z_z)} = 1 - \frac{\bar{I}_{eu}}{\bar{I}_z} (1 - ef_{eu}) \quad (16b)$$

where $\bar{I}_z = \frac{I_m(0, Z_z)}{Z_z}$ represents the averaged effect of light availability on the phytoplankton

growth rate above a fixed depth Z_z . \bar{I}_z decreases with increasing $[Chl]$. $I_m(0, Z_z) =$

$\int_0^{Z_z} I_m(z) dz = -\frac{1}{K_l} \times \ln\left(\frac{I_0 \times e^{-K_l \times Z_z} + k_m^l}{I_0 + k_m^l}\right)$ denotes the integrated effect of light availability on

phytoplankton growth rate above the depth Z_z . The term \bar{I}_z in equation (16) is a function of

the optical depth of Z_z (i.e., $Z_z \times K_l$). ef_z decreases with increasing Z_z , $[Chl]$, and optical

depth ($Z_z \times K_l$) as schematically shown in Figure 2(B). As equation (16) can be rewritten as

$$ef_z = \frac{NCP(0, Z_z)}{NPP(0, Z_z)} = 1 - \frac{HR(0, Z_z)}{NPP(0, Z_z)} = 1 - \frac{\frac{HR(0, Z_z)}{C}}{\frac{NPP(0, Z_z)}{C}},$$

these results can be alternatively explained by the biomass-normalized NPP ($\frac{NPP(0, Z_z)}{C}$) (i.e., the autotrophic growth rate) decreasing with

increasing $[Chl]$ due to light attenuation while the biomass-normalized HR ($\frac{HR(0, Z_z)}{C}$) is

insensitive to changes in $[Chl]$.

3.3. Comparison to other export ratio algorithms

Rearranging and taking the natural logarithm of equation (9) yields:

$$\ln(1 - ef_{eu}) = (B_t - P_t) \times T + \ln(\beta) + \ln\left(\frac{1}{\bar{I}_{eu}}\right) + \ln\left(\frac{1}{N_m}\right) \quad (17)$$

In sum, the controls on the export efficiency can be decomposed into four components: (1)

the temperature dependence of the balance between autotrophic and heterotrophic processes

$((B_t - P_t) \times T)$, (2) the community structure ($\ln(\beta)$), (3) the effect of light availability on the phytoplankton growth rate, and (4) the effect of nutrient availability on the phytoplankton growth rate. Missing or misrepresenting one of these components may impair the accuracy of satellite export production estimates. Equation (17) may be further simplified to:

$$ef_{eu} = -(B_t - P_t) \times T - \ln(\beta) + \ln(\overline{I_{eu}}) + \ln(N_m) \quad (18)$$

based on the rough first-order approximation ($\ln(1 - ef_{eu}) \approx -ef_{eu}$ with increasing errors as $ef_{eu} \rightarrow 1$). If $(B_t - P_t)$ in equation (18) is a constant, ef_{eu} is a negative linear function of temperature, consistent in form with the empirical model of *Dunne et al.* [2005]: $pe_r =$

$$-0.0081 \times T + 0.0668 \times \ln\left(\frac{Chl}{Z_{eu}}\right) + 0.426, \text{ where } pe_r \text{ is the particulate export ratio and } Chl$$

in this case reflects the chlorophyll inventory over the euphotic zone. Alternatively, if the temperature dependence $(B_t - P_t)$ relates to NPP, equation (18) is more in line with the

empirical equations in *Laws et al.* [2011]: $ef = -\frac{0.0165 \times tp}{51.7 + tp} \times T + \frac{0.5857 \times tp}{51.7 + tp}$ and $ef =$

$$-\frac{0.43 \times tp^{0.307}}{30} \times T + 0.04756 \times 0.78 \times tp^{0.307}, \text{ where } tp \text{ is defined as NPP in } Laws \text{ et al.}$$

[2011]. The term $-\ln(\beta)$ in equation (18) may correspond to the $\ln\left(\frac{Chl}{Z_{eu}}\right)$ term in *Dunne et al.* [2005] because β is associated with phytoplankton community structure, which is in turn correlated with $[Chl]$ [*Agawin et al.*, 2000; *Brewin et al.*, 2010; *Sathyendranath et al.*, 2001].

The term $\ln(\overline{I_{eu}})$ varies as a function of I_0 , but also depends on $[Chl]$ when integration is to a fixed depth (equations 14 and 16). The terms $\ln(\overline{I_{eu}})$ and $\ln(N_m)$ are not directly taken into account by some earlier models, but are indirectly taken into account through NPP and $[Chl]$ as in *Dunne et al.* [2005] and *Laws et al.* [2011].

3.4. Comparison of the export ratio at the base of the euphotic layer and at 100 m

As an example of the effect of the depth of integration, we derive a functional relationship between ef_z at 100m (ef_{100}) and at the euphotic depth (ef_{eu}) using equations (9, 14, and 16), noting that our conclusions are valid for any other depths of integration. We select a

rem mineralization length scale of $Z^* = 100$ m, a half-saturation constant for radiation of $k_m^I = 4.1$ Einstein $m^{-2} d^{-1}$, and the monthly climatology of ef_{100} estimated using the algorithm of *Dunne et al.*, [2005]. Monthly climatology of sea surface temperature, chlorophyll a concentration, and photosynthetically active radiation were downloaded from the ocean color website (<https://oceancolor.gsfc.nasa.gov/>). We use these data products to calculate the euphotic depth and ef_{100}/ef_{eu} based on equations (7-8).

When Z_{eu} is deeper than 100 m ($Z_{eu} > 100$), $\frac{1-ef_{100}}{1-ef_{eu}} = \frac{\overline{I_{eu}}}{\overline{I_{100}}} < 1$ can be obtained by reorganizing equations (9 and 16), where $\overline{I_{100}}$ is the averaged effect of light availability on the phytoplankton growth rate above 100 m. This relationship suggests that $\frac{ef_{100}}{ef_{eu}}$ is greater than 1 ($\frac{ef_{100}}{ef_{eu}} > 1$) and rapidly decreases with increasing $[Chl]$ (due to decreasing $\overline{I_{100}}$ but no change in $\overline{I_{eu}}$), as shown in the schematic diagram in Figure 3. In the subtropical gyres, where Z_{eu} is often deeper than 100 m due to extremely low $[Chl]$ (e.g., $[Chl] = 0.01$ $mg\ m^{-3}$ leads to $Z_{eu} = 192.66$ m), ef_{100} could be as much as seven times larger than ef_{eu} (Figure 4).

When Z_{eu} is shallower than 100 m ($Z_{eu} < 100$), a simple reorganization of equation (14) yields $\frac{ef_{100}}{ef_{eu}} = e^{-\frac{100-Z_{eu}}{Z^*}}$. This equation suggests that $\frac{ef_{100}}{ef_{eu}}$ is smaller than 1 ($\frac{ef_{100}}{ef_{eu}} < 1$), and that an increase in $[Chl]$ again decreases Z_{eu} and hence $\frac{ef_{100}}{ef_{eu}}$ (Figure 3). However, $\frac{ef_{100}}{ef_{eu}}$ is less sensitive to changes in $[Chl]$ than when $Z_{eu} > 100$ (Figure 3). For example, ef_{100} is less than half of ef_{eu} in regions with very high $[Chl]$ (e.g., Southern Ocean and coastal regions; $[Chl] = 10$ $mg\ m^{-3}$ gives $Z_{eu} = 11.66$ m and $\frac{ef_{100}}{ef_{eu}} = 0.41$ for $Z^* = 100$ m).

These considerations may in part explain the large discrepancies between satellite algorithms in predictions of export production in the subtropical regions, the Southern Ocean, and the Arctic Ocean [*Li and Cassar*, 2016]. In these regions, extremely low and high $[Chl]$

regimes are observed. Some algorithms predict the ef -ratio at the euphotic depth [Eppley and Peterson, 1979; Laws et al., 2000; Siegel et al., 2014], while others at a given depth such as the mixed layer depth [Li and Cassar, 2016], or 100 m [Dunne et al., 2005; Henson et al., 2011; Le Moigne et al., 2016; Maiti et al., 2013]. Differing integration depths could also explain the reported inconsistent relationship between ef -ratio and GPP [Hendricks et al., 2004] and NPP [Maiti et al., 2013].

ef -ratios measured at different depths display similar functionalities (equations 9, 14, and 16); however, integrating to the euphotic depths may be preferable. First, as opposed to the euphotic depth which has a clear influence on phytoplankton physiology, a physical depth's influence on the ef -ratio changes with light attenuation, preventing the exploration of controls (e.g., plankton community structure) on the ef -ratio across regions with different [Chl]. An ef -ratio measured shallower than the euphotic depth misses parts of the particles produced. Conversely, an ef -ratio measured deeper than the euphotic depth disproportionately reflects particle destruction processes.

There are practical reasons to measure the ef -ratio at depth. For example, shallow sediment traps are notoriously unreliable [Buesseler, 1991]. However, as shown in equation (14), export at depth can be modeled as a function of ef_{eu} and flux attenuation below the euphotic depth, albeit with significant uncertainties. Because controls on the ef_{eu} and the transfer efficiency are likely different [Buesseler and Boyd, 2009; Lima et al., 2014], this two-step approach likely improves predictions of the strength of the biological pump. Our results also underscore Buesseler and Boyd [2009] recommendation to account for variations in Z_{eu} when reporting export or ef -ratios.

4. Influence of environmental properties on the export ratio

In order to gain some quantitative intuition into how N , I_0 , T , $[Chl]$, and MLD influence the ef -ratio, we take the partial derivative of ef_z at the base of the mixed layer (ef_{ml}) relative to each property in equation (16):

$$\frac{\partial ef_{ml}}{\partial N} = N_m \times \frac{k_m^N}{N^2} \times (1 - ef_{ml}) \quad (19)$$

$$\frac{\partial ef_{ml}}{\partial I_0} = \frac{I_m(MLD) \times (e^{K_I \times MLD} - 1)}{I_m(0, MLD) \times K_I} \times \frac{k_m^I}{(I_0 + k_m^I) \times I_0} \times (1 - ef_{ml}) \quad (20)$$

$$\frac{\partial ef_{ml}}{\partial T} = -(B_t - P_t) \times (1 - ef_{ml}) \quad (21)$$

$$\frac{\partial ef_{ml}}{\partial [Chl]} = - \left(1 - \frac{I_m(MLD)}{\bar{I}_{ml}} \right) \times \frac{1}{K_I} \times \frac{dK_I}{d[Chl]} \times (1 - ef_{ml}) \quad (22)$$

$$\frac{\partial ef_{ml}}{\partial MLD} = - \left(1 - \frac{I_m(MLD)}{\bar{I}_{ml}} \right) \times \frac{1}{MLD} \times (1 - ef_{ml}) \quad (23)$$

where $I_m(MLD) = \frac{I_0 \times e^{-K_I \times MLD}}{I_0 \times e^{-K_I \times MLD} + k_m^I}$ represents the influence of light availability on phytoplankton growth rate at MLD ; $\bar{I}_{ml} = \frac{I_m(0, MLD)}{MLD}$ represents the averaged effect of light availability on the phytoplankton growth rate within the mixed layer; $I_m(0, MLD)$ is the integrated effect of light availability on the phytoplankton growth rate over the mixed layer; and $\frac{dK_I}{d[Chl]}$ can be derived from equation (5) and is positive ($\frac{dK_I}{d[Chl]} > 0$). The derivations of equations (19-23) are presented in the supplementary material. ef_{ml} increases with N ($\frac{\partial ef_{ml}}{\partial N} > 0$) and I_0 ($\frac{\partial ef_{ml}}{\partial I_0} > 0$) due to increasing phytoplankton growth rate. ef_{ml} decreases with T ($\frac{\partial ef_{ml}}{\partial T} < 0$) because of the higher temperature sensitivity of heterotrophic respiration compared to phytoplankton growth rate ($B_t > P_t$), in line with multiple previous studies [Cael and Follows, 2016; Dunne et al., 2005; Henson et al., 2011; Laws et al., 2011; Laws et al., 2000]. ef_{ml} decreases with $[Chl]$ ($\frac{\partial ef_{ml}}{\partial [Chl]} < 0$) and MLD ($\frac{\partial ef_{ml}}{\partial MLD} < 0$) due to decreasing average light availability. In reality, a deepening of the mixed layer may also entrain nutrients

from the subsurface, leading to an increase in ef_{ml} (equation (19)). This effect is not directly taken into account in our model. The balance of the effects of *MLD* deepening on nutrient and light availability ultimately determines how ef_{ml} varies with *MLD*. Equations (19-23) can be applied to ef_{eu} , with the exception that ef_{eu} is independent of $[Chl]$ and the depth of integration ($\frac{\partial ef_{eu}}{\partial [Chl]} = \frac{\partial ef_{eu}}{\partial Z_{eu}} = 0$). In some studies, ef_z is derived from taking the ratio of export (or NCP) measurements integrated to a certain depth (e.g., 100m or *MLD*) to NPP integrated over the euphotic depth. Under such circumstances, the sign of $\frac{\partial ef_z}{\partial [Chl]}$ varies, with ef -ratio displaying a bell-shaped relation to $[Chl]$ (see Figure S1 in supplementary material).

4.1. Relation between the export ratio at a fixed depth and net primary production

Recent studies have reported a negative relation between NPP and ef_{100} in the Southern Ocean [Le Moigne *et al.*, 2016; Maiti *et al.*, 2013], in contrast to earlier studies [Dunne *et al.*, 2005; Eppley and Peterson, 1979; Laws *et al.*, 2011; Laws *et al.*, 2000]. Relating the ef -ratio to NPP could lead to spurious negative correlations of the type x vs. (a/x) where “a” is a constant. This is especially the case for deep depths of integration because geographical variability in export production decreases with increasing depth [Antia *et al.*, 2001; Henson *et al.*, 2012]. While we cannot rule out that the negative correlation between the ef -ratio and NPP results from a mathematical tautology, others have hypothesized that it results from grazing and fecal-mediated export [Cavan *et al.*, 2017; Le Moigne *et al.*, 2016], temperature [Henson *et al.*, 2015], and DOC export [Hansell *et al.*, 2009; Maiti *et al.*, 2013]. Many of these factors are encapsulated in the β term relating r_{HR} to μ_{max} in equation (12). β reflects community structure that is in turn related $[Chl]$ and NPP [Lopez-Urrutia *et al.*, 2006]. While the cause remains unknown, our models provide an additional explanation for the reported discrepancies in the relationship between ef_{100} and NPP. NPP is the product of phytoplankton biomass (C) and growth rate (μ). All other factors equal, euphotic-depth

integrated NPP is a positive function of C (Figure 1). Since ef_{100} is a negative function of $[Chl]$, an increase in NPP due to high C will decrease ef_{100} (Figure 2). Conversely, if the increase in NPP stems from other factors such as increasing nutrient and light availability (i.e., higher autotrophic growth rate), ef_{100} is expected to positively correlate with NPP.

4.2. Seasonal variability in the export ratio at the base of the mixed layer

Based on equations (19-23), we decompose the seasonal controls on ef_{ml} as the sum of partial differentials:

$$\Delta ef_{ml} = \frac{\partial ef_{ml}}{\partial N} \times \Delta N + \frac{\partial ef_{ml}}{\partial I_0} \times \Delta I_0 + \frac{\partial ef_{ml}}{\partial T} \times \Delta T + \frac{\partial ef_{ml}}{\partial [Chl]} \times \Delta [Chl] + \frac{\partial ef_{ml}}{\partial MLD} \times \Delta MLD \quad (24)$$

where Δef_{ml} denotes the total differential of ef_{ml} ; and ΔN , ΔI_0 , ΔT , $\Delta [Chl]$, and ΔMLD represent changes in N , I_0 , T , $[Chl]$, and MLD , respectively. As $1 - ef_{ml}$ appears in all the individual equations (19-23), it is not required to estimate the relative contribution of each term in equation (24). We estimate I_0 , T , and $[Chl]$ from satellite data, MLD from the climatology of *de Boyer Montegut et al.* [2004], and N from World Ocean Atlas monthly climatologies [*Garcia et al.*, 2014]. Details on data and the derivation of seasonal changes in nutrient availability are presented in the supplementary material [*Boyd et al.*, 2000; *Boyd and Ellwood*, 2010; *Cassar et al.*, 2007; *Deutsch et al.*, 2007; *Johnson et al.*, 1997; *Martin et al.*, 1990; *Mitchell et al.*, 1991a, *Mitchell et al.*, 1991b; *Moore et al.*, 2013; *Nelson et al.*, 1991; *Sarmiento and Gruber*, 2006]. Figure 5 shows how seasonal variations in ef_{ml} are impacted by I_0 , MLD , T , $[Chl]$, and N . Among these factors, I_0 and MLD dominate seasonal variability in ef_{ml} at high-latitude. In the spring, ef_{ml} sharply increases with increasing I_0 and shoaling MLD ($\frac{\partial ef_{ml}}{\partial I_0} \times \Delta I_0 > 0$ and $\frac{\partial ef_{ml}}{\partial MLD} \times \Delta MLD > 0$). In contrast, decreasing I_0 and deepening MLD in the autumn lead to a decrease in ef_{ml} ($\frac{\partial ef_{ml}}{\partial I_0} \times \Delta I_0 < 0$ and $\frac{\partial ef_{ml}}{\partial MLD} \times \Delta MLD < 0$). Our

results are consistent with the dominant controls of MLD and I_0 on NCP in the Southern Ocean on seasonal timescales [Li, 2017].

T also contributes to the seasonal variability in ef_{ml} . Interestingly, $\frac{\partial ef_{ml}}{\partial T} \times \Delta T$ is higher in polar regions. Similarly, $[Chl]$ affects the seasonality in ef_{ml} north $45^\circ N$ in March and April. However, $\frac{\partial ef_{ml}}{\partial [Chl]} \times \Delta [Chl]$ shows large spatial variability (see the supplementary material).

Conversely, N mostly impacts the seasonality of ef_{ml} in the Southern Ocean. $\frac{\partial ef_{ml}}{\partial N} \times \Delta N$ leads to an increase in ef_{ml} in late austral summer early autumn due to deepening mixed layers, in part counteracting the decreasing light availability associated with I_0 and deepening mixed layers. Additionally, our data support equation (19)'s prediction that ef_{ml} is particularly sensitive to variations in nutrient availability when nutrient concentrations are low (see supplementary material). Because of the assumptions going into the derivation of N , it is likely the parameter with the most uncertain effect on ef_{ml} . Uncertainties, assumptions and simplifications associated with $\frac{\partial ef_{ml}}{\partial N} \times \Delta N$ are discussed in the section on caveats and limitations. Overall, our results emphasize that caution should be exercised when interpreting ef_{ml} across regions and seasons because of varying I_0 , MLD , T , $[Chl]$, and N .

5. Caveats, limitations, additional considerations, and future improvements

Below we enumerate some of the assumptions and simplifications that go into the construction of our model. While they introduce uncertainties, they do not change our main conclusions that fundamental factors confound the interpretation of the ef -ratio.

Photophysiology: Modeling the influence of light availability on phytoplankton growth assuming Michaelis-Menten kinetics does not account for light inhibition and photoacclimation [Geider, 1987; Geider et al., 1996; Geider et al., 1998; Jassby and Platt, 1976; Pahlow and Oschlies, 2009]. In addition, K_I varies with depth due to the optional attenuation of PAR (see Li and Cassar [2017] and references therein), with the relationship

between K_I and $[Chl]$ also being impacted by other factors, including detritus, colored dissolved organic matter, and solar zenith angle [Gordon, 1989]. We also note that defining the euphotic depth based on a percentage of surface irradiance has been shown to be of little physiological significance [Banse, 2004; Laws *et al.*, 2014; Letelier *et al.*, 2004; Lorenzen, 1976; Marra *et al.*, 2014]. While our model can readily be adapted to reflect a depth more meaningful to photochemistry, for the purpose of this study, the definition in equation (8) is adequate.

Stoichiometry: The elemental stoichiometry and half-saturation constants of marine phytoplankton are known to vary with seasonal changes in growth conditions and species [Eppley *et al.*, 1969; Moreno and Martiny, 2018; Smith *et al.*, 2009]. Our model does not account for this variability and assumes that the concentrations and half-saturation constants of limiting and non-limiting factors vary proportionally. All these simplifications and top-down controls on the phytoplankton growth rate (as opposed to nutrients) will need to be further evaluated.

Other biogeochemical and trophic processes: By design, our metabolism-based model prescinds complex biogeochemical processes represented in food-web models. While our modeling of autotrophy is on par with more complex food web models (e.g., NPZD), our representation of heterotrophy being a simple function of temperature and biomass does not reflect the panoply of biogeochemical and trophic processes influencing organic carbon loss from the system. For example, our model does not represent the process of particle aggregation, which is believed to be a first-order control on the ef -ratio [Boyd and Trull, 2007; Burd and Jackson, 2009; Passow *et al.*, 1994]. Aggregation with rapid sinking would lead to lower surface respiration and higher ef -ratios than predicted based on the model's temperature parameterization. The temperature dependence of r_{HR} and μ_{max} have large uncertainties (see Li and Cassar [2017] and references therein). Variations in the relative

proportion of POC and DOC production associated with NCP, attributed to food web processes and plankton's physiological status [Emerson, 2014; Hansell and Carlson, 1998; Hygum et al., 1997; Thornton, 2014], are also not included in our modeling effort.

Our model assumes steady-state. A lack of steady-state may lead to two types of biases, natural and methodological. First, export efficiency observations may be biased when export lags production [Buesseler, 1998; Buesseler et al., 2009; Henson et al., 2015], in which case the *ef*-ratio would be under(over)-estimated in the production (export) phase. This is particularly important in physically dynamic and biologically sluggish (low temperature) systems such as the Southern Ocean. Second, differences in integration timescales of export production and NPP bias estimates of the *ef*-ratio in systems that are not at steady-state. For example, export production measurements (~24 days based on ²³⁴Th) usually have longer integration timescales than NPP estimates (~1 day).

Vertical profiles: For simplicity, we assume that μ_{max} , r_{HR} , N , k_m^N , k_m^I , $[Chl]$, and C are well mixed or constant within the euphotic zone and mixed layer. However, these parameters may vary within the mixed layer, especially for water columns with limited turbulent mixing. In the subtropical regions where the water column is well stratified, low nutrient availability often leads to euphotic zones that are deeper than the mixed layer, and as a result some parameters (e.g., N , $[Chl]$, and C) beneath the mixed layer may differ from those within the mixed layer.

6. Conclusions

In this study, we developed a metabolism-based mechanistic model to explore how fundamental factors may confound the interpretation of field observations of the export ratio (*ef*-ratio). Our results show that the effect of trophic processes and community composition on the export efficiency may be masked by changes in temperature, biomass and light availability. As such, analyses of the impact of biological and biogeochemical processes on

ef_{ml} should be interpreted with caution, especially in high latitudes where variations in ef_{ml} are dominated by mixed-layer depth and surface radiation over seasonal timescales. Our approach also offers a new framework for relating phytoplankton size composition to field estimates, satellite algorithms and earth-system models of the ef -ratio. Finally, our theoretical considerations provide further support for reporting or normalizing field observations of the ef -ratio to the euphotic depth. While the best depth horizon for reporting ef -ratio may depend on the process under study, our modeling effort shows that estimating ef -ratios at a depth other than the euphotic depth (e.g., 100m or MLD) complicates the interpretation of the temporal and spatial variability in the ef -ratio.

More fundamentally, our study demonstrates that it may be time to revisit the export ratio proxy. In their classical paper, *Eppley and Peterson* [1979] first recommended normalizing new production to primary production (f-ratio) as the “total flux seems to be approximately proportional to the plankton production in the overlying water”. While normalization by ratio correction is commonly applied in life sciences to account for the effect of a confounding variable, it is known to be flawed (*Karp et al.*, [2012] and references therein). In addition to the issues associated with ratio corrections, our theoretical considerations above demonstrate that export is not a simple function of NPP. Identical NPP resulting from differing autotrophic biomass and growth rates may lead to differing export ratios. These mathematical and biogeochemical shortcomings with the export ratio thus argue for the development of more ecumenical proxies of the biological pump.

Acknowledgements

ZL was supported by a NASA Earth and Space Science Fellowship (Grant No. NNX13AN85H) and the Postdoctoral Scholarship Program at Woods Hole Oceanographic Institution. NC was supported by NASA Grant 5109296. Satellite data, nutrient concentration,

and monthly MLD climatology are downloaded from NASA ocean color

(<http://oceancolor.gsfc.nasa.gov/cms/>), World Ocean Atlas

(<https://www.nodc.noaa.gov/OC5/woa13/>), and

<http://www.ifremer.fr/cerweb/deboyer/mld/home.php>, respectively.

References

Agawin, N. S. R., C. M. Duarte, and S. Agusti (2000), Nutrient and temperature control of the contribution of picoplankton to phytoplankton biomass and production, *Limnol. Oceanogr.*, 45, 591-600.

Aksnes, D. L., and P. Wassmann (1993), Modeling the significance of zooplankton grazing for export production, *Limnol. Oceanogr.*, 38, 978-985.

Allredge, A. L., and M. W. Silver (1988), Characteristics, dynamics and significance of marine snow, *Progress in Oceanography*, 20(1), 41-82.

Antia, A. N., et al. (2001), Basin-wide particulate carbon flux in the Atlantic Ocean: Regional export patterns and potential for atmospheric CO₂ sequestration, *Global Biogeochem. Cycles*, 15(4), 845–862, doi:10.1029/2000GB001376.

Armstrong, R. A., C. Lee, J. I. Hedges, S. Honjo, and S. G. Wakeham (2002), A new, mechanistic model for organic carbon fluxes in the ocean based on the quantitative association of POC with ballast minerals, *Deep-Sea Res Pt Ii*, 49(1-3), 219-236.

Arrigo, K. R., G. L. van Dijken, and S. Bushinsky (2008), Primary production in the Southern Ocean, 1997–2006, *J. Geophys. Res.*, 113, C08004, doi:10.1029/2007JC004551.

Baines, S. B., M. L. Pace, and D. M. Karl (1994), Why does the relationship between sinking flux and planktonic primary production differ between lakes and oceans, *Limnology and Oceanography*, 39(2), 213-226.

Banse, K. (2004), Should we continue to use the 1% light depth convention for estimating the compensation depth of phytoplankton for another 70 years? *Limnology and Oceanography Bulletin*, 13, 49-51.

- Betzer, P. R., W. J. Showers, E. A. Laws, C. D. Winn, G. R. Ditullio, and P. M. Kroopnick (1984), Primary productivity and particle fluxes on a transect of the equator at 153°W in the Pacific Ocean, *Deep-Sea Research Part A.*, 31(1), 1-11.
- Boyd, P., and P. Newton (1995), Evidence of the potential influence of planktonic community structure on the interannual variability of particulate organic carbon flux, *Deep Sea Research Part I*, 42(5), 619-639.
- Boyd, P. W., and P. P. Newton (1999), Does planktonic community structure determine downward particulate organic carbon flux in different oceanic provinces? *Deep-Sea Res Pt I*, 46(1), 63-91.
- Boyd, P. W., and T. W. Trull (2007), Understanding the export of biogenic particles in oceanic waters: Is there consensus? *Progress in Oceanography*, 72(4), 276-312.
- Boyd, P. W., et al. (2000), A mesoscale phytoplankton bloom in the polar Southern Ocean stimulated by iron fertilization, *Nature*, 407, 695–702.
- Boyd, P. W., and M. J. Ellwood (2010), The biogeochemical cycle of iron in the ocean, *Nat. Geosci.*, 3, 675–682, doi:10.1038/ngeo964.
- Brewin, R. J. W., S. Sathyendranath, T. Hirata, S. J. Lavender, R. Barciela, and N. J. Hardman-Mountford (2010), A three-component model of phytoplankton size class for the Atlantic Ocean, *Ecological Modelling*, 221, 1472–1483.
- Britten, G. L., L. Wakamatsu, and F. W. Primeau (2017), The temperature-ballast hypothesis explains carbon export efficiency observations in the Southern Ocean, *Geophys Res Lett*, 2016GL072378.
- Buesseler, K. O. (1991), Do upper-ocean sediment traps provide an accurate record of particle flux? *Nature*, 353, 420-423.
- Buesseler, K. O. (1998), The decoupling of production and particulate export in the surface ocean, *Global Biogeochem Cy*, 12(2), 297-310.
- Buesseler, K. O., and P. W. Boyd (2009), Shedding light on processes that control particle export and flux attenuation in the twilight zone of the open ocean, *Limnology and Oceanography*, 54(4), 1210-1232.

- Buesseler, K. O., S. Pike, K. Maiti, C. H. Lamborg, D. A. Siegel, and T. W. Trull (2009), Thorium- 234 as a tracer of spatial, temporal and vertical variability in particle flux in the North Pacific, *Deep Sea Res., Part I*, 56(7), 1143–1167, doi:10.1016/j.dsr.2009.04.001.
- Burd, A. B., and G. A. Jackson (2009), Particle aggregation, *Annu Rev Mar Sci*, 1, 65-90.
- Cael, B. B., and M. J. Follows (2016), On the temperature dependence of oceanic export efficiency, *Geophys Res Lett*, 43(10), 5170-5175.
- Cassar, N., M. L. Bender, B. A. Barnett, S. Fan, W. J. Moxim, H. Levy, and B. Tilbrook (2007), The Southern Ocean biological response to aeolian iron deposition, *Science*, 317, 1067–1070, doi:10.1126/science.1144602.
- Cavan, E. L., S. A. Henson, A. Belcher, and R. Sanders (2017), Role of zooplankton in determining the efficiency of the biological carbon pump, *Biogeosciences*, 14(1), 177-186.
- Cavan, E. L., F. A. C. Le Moigne, A. J. Poulton, G. A. Tarling, P. Ward, C. J. Daniels, G. M. Fragoso, and R. J. Sanders (2015), Attenuation of particulate organic carbon flux in the Scotia Sea, Southern Ocean, is controlled by zooplankton fecal pellets, *Geophys Res Lett*, 42(3), 821-830.
- de Boyer Montegut, C., G. Madec, A. S. Fischer, A. Lazar, and D. Iudicone (2004), Mixed layer depth over the global ocean: An examination of profile data and a profile-based climatology, *Journal of Geophysical Research-Oceans*, 109(C12).
- Deutsch, C., J. L. Sarmiento, D. M. Sigman, N. Gruber, and J. P. Dunne (2007), Spatial coupling of nitrogen inputs and losses in the ocean, *Nature*, 445(7124), 163-167.
- Dugdale, R. C., and J. J. Goering (1967), Uptake of new and regenerated forms of nitrogen in primary productivity, *Limnology and Oceanography*, 12(2), 196-206.
- Dunne, J. P., R. A. Armstrong, A. Gnanadesikan, and J. L. Sarmiento (2005), Empirical and mechanistic models for the particle export ratio, *Global Biogeochem Cy*, 19(4).
- Dutkiewicz, S., M. Follows, J. Marshall, and W. W. Gregg (2001), Interannual variability of phytoplankton abundances in the North Atlantic, *Deep-Sea Res Pt II*, 48(10), 2323-2344.
- Emerson, S. (2014), Annual net community production and the biological carbon flux in the ocean, *Global Biogeochem. Cycles*, 28, 14–28, doi:10.1002/2013GB004680.
- Eppley, R. W. (1972), Temperature and phytoplankton growth in the sea, *Fishery Bulletin*, 70(4), 1063-1085.

- Eppley, R. W., and B. J. Peterson (1979), Particulate organic matter flux and planktonic new production in the deep ocean, *Nature*, 282, 677-680.
- Eppley, R. W., J. N. Rogers, and J. J. McCarthy (1969), Half-saturation constants for uptake of nitrate and ammonium by marine phytoplankton, *Limnology and Oceanography*, 14(6), 912-920.
- Francois, R., S. Honjo, R. Krishfield, and S. Manganini (2002), Factors controlling the flux of organic carbon to the bathypelagic zone of the ocean, *Global Biogeochem Cy*, 16(4).
- Garcia, H. E., R. A. Locarnini, T. P. Boyer, J. I. Antonov, O. K. Baranova, M. M. Zweng, J. R. Reagan, and D. R. Johnson (2014), *World Ocean Atlas 2013, Volume 4: Dissolved Inorganic Nutrients (phosphate, nitrate, silicate)*, S. Levitus, Ed., A. Mishonov Technical Ed.; NOAA Atlas NESDIS 76, 25 pp.
- Geider, R. J. (1987), Light and temperature-dependence of the carbon to chlorophyll-a ratio in microalgae and cyanobacteria: Implications for physiology and growth of phytoplankton, *New Phytol*, 106(1), 1-34.
- Geider, R. J., H. L. MacIntyre, and T. M. Kana (1996), A dynamic model of photoadaptation in phytoplankton, *Limnology and Oceanography*, 41(1), 1-15.
- Geider, R. J., H. L. MacIntyre, and T. M. Kana (1998), A dynamic regulatory model of phytoplanktonic acclimation to light, nutrients, and temperature, *Limnology and Oceanography*, 43(4), 679-694.
- Gordon, H. R. (1989), Can the Lambert-Beer law be applied to the diffuse attenuation coefficient of ocean water? *Limnol. Oceanogr.*, 34, 1389– 1409.
- Guidi, L., et al. (2016), Plankton networks driving carbon export in the oligotrophic ocean, *Nature*, 532(7600), 465-470.
- Hansell, D. A., C. A. Carlson, D. J. Repeta, and R. Schlitzer (2009), Dissolved organic matter in the ocean a controversy stimulates new insights, *Oceanography*, 22(4), 202-211.
- Hansell, D. A., and C. A. Carlson (1998), Net community production of dissolved organic carbon, *Global Biogeochem. Cycles*, 12, 443–453.
- Hendricks, M. B., M. L. Bender, and B. A. Barnett (2004), Net and gross O₂ production in the Southern Ocean from measurements of biological O₂ saturation and its triple isotope composition, *Deep Sea Res. Part I*, 51, 1541–1561.

- Henson, S. A., A. Yool, and R. Sanders (2015), Variability in efficiency of particulate organic carbon export: A model study, *Global Biogeochem Cy*, 29(1), 33-45.
- Henson, S. A., R. Sanders, and E. Madsen (2012), Global patterns inefficiency of particulate organic carbon export and transfer to the deep ocean, *Global Biogeochem. Cycles*, 26, doi: 10.1029/2011GB004099.
- Henson, S. A., R. Sanders, E. Madsen, P. J. Morris, F. Le Moigne, and G. D. Quartly (2011), A reduced estimate of the strength of the ocean's biological carbon pump, *Geophys Res Lett*, 38(4).
- Huang, K., H. Ducklow, M. Vernet, N. Cassar, and M. L. Bender (2012), Export production and its regulating factors in the West Antarctica Peninsula region of the Southern Ocean, *Global Biogeochem Cy*, 26(2).
- Huisman, J., and F. J. Weissing (1994), Light-limited growth and competition for light in well-mixed aquatic environments: An elementary model, *Ecology*, 75(2), 507-520.
- Hygum, B.H., J.W. Petersen, and M. Søndergaard (1997), Dissolved organic carbon released by zooplankton grazing activity - a high quality substrate pool for bacteria, *Journal of Plankton Research*, 19, 97-111
- Jackson, G.A., and T. Kiørboe (2008), Maximum phytoplankton concentrations in the sea. *Limnol. Oceanogr.*, 53, 395–399.
- Jakobsen, H. H., and S. Markager (2016), Carbon-to-chlorophyll ratio for phytoplankton in temperate coastal waters: Seasonal patterns and relationship to nutrients, *Limnol. Oceanogr.*, 61, 1853–1868.
- Jassby, A. D., and T. Platt (1976), Mathematical formulation of the relationship between photosynthesis and light for phytoplankton, *Limnology and Oceanography*, 21(4), 540-547.
- Johnson, K. S., R. M. Gordon, K. H. Coale (1997), What controls dissolved iron concentrations in the world ocean?, *Mar. Chem.*, 57, 137–161.
- Karp N. A., A. Segonds-Pichon, A. K. Gerdin, R. Ramírez-Solis, J. K. White (2012), The fallacy of ratio correction to address confounding factors, *Lab Anim*, 46, 245-252.

Klaas, C., and D. E. Archer (2002), Association of sinking organic matter with various types of mineral ballast in the deep sea: Implications for the rain ratio, *Global Biogeochem Cy*, 16(4).

Laurenceau-Cornec, E. C., et al. (2015), The relative importance of phytoplankton aggregates and zooplankton fecal pellets to carbon export: insights from free-drifting sediment trap deployments in naturally iron-fertilised waters near the Kerguelen Plateau, *Biogeosciences*, 12(4), 1007-1027.

Laws, E. A. (2013), Evaluation of in situ phytoplankton growth rates: A synthesis of data from varied approaches, *Annual Review of Marine Science*, 5(5), 247-268.

Laws, E. A., E. D'Sa, and P. Naik (2011), Simple equations to estimate ratios of new or export production to total production from satellite-derived estimates of sea surface temperature and primary production, *Limnol Oceanogr-Meth*, 9(13), 593-601.

Laws, E. A., P. G. Falkowski, W. O. Smith, H. Ducklow, and J. J. McCarthy (2000), Temperature effects on export production in the open ocean, *Global Biogeochem Cy*, 14(4), 1231-1246.

Laws, E. A., R. M. Letelier, and D. M. Karl (2014), Estimating the compensation irradiance in the ocean: The importance of accounting for non- photosynthetic uptake of inorganic carbon, *Deep Sea Res., Res. I*, 93, 35–40, doi:10.1016/j.dsr.2014.07.011

Le Moigne, F. A. C., S. A. Henson, E. Cavan, C. Georges, K. Pabortsava, E. P. Achterberg, E. Ceballos-Romero, M. Zubkov, and R. J. Sanders (2016), What causes the inverse relationship between primary production and export efficiency in the Southern Ocean? *Geophys Res Lett*, 43(9), 4457-4466.

Letelier, R. M., D. M. Karl, M. R. Abbott, and R. R. Bidigare (2004), Light driven seasonal patterns of chlorophyll and nitrate in the lower euphotic zone of the North Pacific Subtropical Gyre, *Limnol. Oceanogr.*, 49(2), 508–519

Li, Z. (2017), Remotely sensed estimates and controls of large-scale oceanic net community production, PhD dissertation, Duke University, ProQuest Dissertations Publishing, 10258797.

Li, Z., and N. Cassar (2016), Satellite estimates of net community production based on O₂/Ar observations and comparison to other estimates, *Global Biogeochem Cy*, 30(5), 735-752.

- Li, Z., and N. Cassar (2017), A mechanistic model of an upper bound on oceanic carbon export as a function of mixed layer depth and temperature, *Biogeosciences*, 14, 5015-5027, doi:10.5194/bg-14-5015-2017.
- Lima, I. D., P. J. Lam, and S. C. Doney (2014), Dynamics of particulate organic carbon flux in a global ocean model, *Biogeosciences*, 11, 1177–1198, doi:10.5194/bg-11-1177-2014.
- Lopez-Urrutia, A., E. San Martin, R. P. Harris, and X. Irigoien (2006), Scaling the metabolic balance of the oceans, *P Natl Acad Sci USA*, 103(23), 8739-8744.
- Lorenzen, C.J. (1976), Primary production in the sea, D.H. Cushing, J.J. Walsh (Eds.), *Ecology of the Seas*, Blackwell Scientific Publications, Oxford, 173-185
- Lutz, M., R. Dunbar, and K. Caldeira (2002), Regional variability in the vertical flux of particulate organic carbon in the ocean interior, *Global Biogeochem Cy*, 16(3).
- Maiti, K., M. A. Charette, K. O. Buesseler, and M. Kahru (2013), An inverse relationship between production and export efficiency in the Southern Ocean, *Geophys Res Lett*, 40(8), 1557-1561.
- Marra, J.F., V.P. Lance, R.D. Vaillancourt, B.R. Hargreaves (2014), Resolving the ocean's euphotic zone, *Deep Sea Res. Part I*, 83, 45-50
- Martin, J. H., G. A. Knauer, D. M. Karl, and W. W. Broenkow (1987), Vertex - Carbon Cycling in the Northeast Pacific, *Deep-Sea Res*, 34(2), 267-285.
- Martin, J. H., R. M. Gordon, and S. E. Fitzwater (1990), Iron in Antarctic waters, *Nature*, 345(6271), 156-158.
- Michaels, A. F., and M. W. Silver (1988), Primary production, sinking fluxes and the microbial food web, *Deep-Sea Res*, 35(4), 473-490.
- Mitchell, B. G., and O. Holm-Hansen (1991), Observations and modeling of the Antarctic phytoplankton crop in relation to mixing depth, *Deep-Sea Res*, 38(8-9), 981-1007.
- Mitchell, B. G., E. A. Brody, O. Holm-Hansen, C. McClain, and J. Bishop (1991), Light limitation of phytoplankton biomass and macronutrient utilization in the Southern Ocean, *Limnology and Oceanography*, 36(8), 1662-1677.
- Moore, C. M., et al. (2013), Processes and patterns of oceanic nutrient limitation, *Nat. Geosci.*, doi:10.1038/ngeo1765.

- Morel A., Huot Y., Gentili B., Werdell P.J., Hooker S.B., Franz, B.A. (2007), Examining the consistency of products derived from various ocean sensors in open ocean (Case 1) waters in the perspective of a multi-sensor approach, *Remote Sens. Environ.*, 111, 69-88
- Moreno, A. R., and Martiny, A. C. (2018), Ecological stoichiometry of ocean plankton. *Annu. Rev. Mar. Sci.* 10, 1–27. doi:10.1146/annurev-marine-121916-063126
- Murray, J. W., J. Young, J. Newton, J. Dunne, T. Chapin, B. Paul, and J. J. McCarthy (1996), Export flux of particulate organic carbon from the central equatorial Pacific determined using a combined drifting trap-²³⁴Th approach, *Deep Sea Res., Part II*, 43, 1095-1132
- Nelson, D. M., and W. O. Smith (1991), Sverdrup revisited: Critical depths, maximum chlorophyll levels, and the control of Southern Ocean productivity by the irradiance-mixing regime, *Limnology and Oceanography*, 36(8), 1650-1661.
- Pahlow M., and A. Oschlies (2009), Chain model of phytoplankton P, N and light colimitation, *Mar Ecol Prog Ser*, 376, doi:10.3354/meps07748
- Palevsky, H. I., and S.C. Doney (2018), How choice of depth horizon influences the estimated spatial patterns and global magnitude of ocean carbon export flux, *Geophysical Research Letters*, 45, doi:10.1029/2017GL076498
- Passow, U., A. L. Alldredge, and B. E. Logan (1994), The role of particulate carbohydrate exudates in the flocculation of diatom blooms, *Deep-Sea Res Pt I*, 41(2), 335-357
- Rivkin, R. B., and L. Legendre (2001), Biogenic carbon cycling in the upper ocean: Effects of microbial respiration, *Science*, 291(5512), 2398-2400.
- Sarmiento, J. L., and N. Gruber (2006), *Ocean Biogeochemical Dynamics*, Princeton Univ. Press, Princeton, N. J.
- Sathyendranath, S., V. Stuart, G. Cota, H. Mass, and T. Platt (2001), Remote sensing of phytoplankton pigments: A comparison of empirical and theoretical approaches, *International Journal of Remote Sensing*, 22, 249–273.
- Siegel, D. A., K. O. Buesseler, S. C. Doney, S. F. Sailley, M. J. Behrenfeld, and P. W. Boyd (2014), Global assessment of ocean carbon export by combining satellite observations and food-web models, *Global Biogeochem Cy*, 28(3), 181-196.

Smith S. L., Y. Yamanaka, M. Pahlow, A. Oschlies (2009), Optimal uptake kinetics: physiological acclimation explains the pattern of nitrate uptake by phytoplankton in the ocean, *Mar Ecol Prog Ser* 384, doi:10.3354/meps08022

Thornton, D. C. O. (2014), Dissolved organic matter (DOM) release by phytoplankton in the contemporary and future ocean, *Eur. J. Phycol.*, 49 (1), 20-46, doi:10.1080/09670262.2013.875596

Accepted Article

Table 1. Model parameters, abbreviations, and units

Parameter	Description	Units
MLD	Mixed layer depth	m
Z_{eu}	Euphotic depth	m
Z_z	A fixed depth	m
z	Depth	m
NPP(z)	Net primary production at depth z	mmol C m ⁻³ d ⁻¹
NPP(0,z)	Net primary production above depth z	mmol C m ⁻² d ⁻¹
HR(z)	Heterotrophic respiration at depth z	mmol C m ⁻³ d ⁻¹
HR(0,z)	Heterotrophic respiration above depth z	mmol C m ⁻² d ⁻¹
NCP(z)	Net community production at depth z	mmol C m ⁻³ d ⁻¹
NCP(0,z)	Net community production above depth z	mmol C m ⁻² d ⁻¹
F	Export production	mmol C m ⁻² d ⁻¹
$ef_z, ef_{eu}, ef_{100}, ef_{ml}$	ef_z is the export ratio at any depth z, which includes the specific cases of ef_z at the euphotic depth (ef_{eu}), 100m (ef_{100}), and mixed layer depth (ef_{ml}).	unitless
N	Nutrient concentration	mmol m ⁻³
k_m^N	Half-saturation constant for nutrient concentration	mmol m ⁻³
N_m	Nutrient effect on the phytoplankton growth $N_m = \frac{N}{N+k_m^N}$	unitless
PAR	Photosynthetically active radiation	Einstein m ⁻² d ⁻¹
I_0	Photosynthetically active radiation just beneath water surface	Einstein m ⁻² d ⁻¹
$I(z)$	Photosynthetically active radiation at depth z	Einstein m ⁻² d ⁻¹
k_m^I	Half-saturation constant for PAR (4.1 einstein m ⁻² d ⁻¹ , Behrenfeld and Falkowski [1997])	Einstein m ⁻² d ⁻¹
$I_m(z)$	Light effect on the phytoplankton growth at depth z, $I_m(z) = \frac{I(z)}{I(z)+k_m^I} = \frac{I_0 \times e^{-K_I \times z}}{I_0 \times e^{-K_I \times z} + k_m^I}$	unitless
$I_m(0, z)$	Integrated light effect on phytoplankton growth above depth z, $I_m(0, z) = -\frac{1}{K_I} \times \ln\left(\frac{I_0 \times e^{-K_I \times z} + k_m^I}{I_0 + k_m^I}\right)$	unitless
$\bar{I}_z, \bar{I}_{eu}, \bar{I}_{100}, \bar{I}_{ml}$	\bar{I}_z represents the averaged effect of light availability on the phytoplankton growth rate within the depth z, which includes the specific cases of \bar{I}_z at the euphotic depth (\bar{I}_{eu}), 100m (\bar{I}_{100}), and mixed layer depth (\bar{I}_{ml}).	unitless
μ_{max}	Maximum phytoplankton specific growth rate	d ⁻¹
r_{HR}	Heterotrophic respiration specific rate	d ⁻¹
K_I	Diffusion attenuation coefficient	m ⁻¹
$K_I(490)$	Diffusion attenuation coefficient at 490 nm	m ⁻¹
C	Phytoplankton biomass concentration	mmol m ⁻³
[Chl]	Chlorophyll a concentration	mg m ⁻³
POC	Particulate organic carbon	mg m ⁻³
DOC	Dissolved organic carbon	mg m ⁻³
T	Sea surface temperature	°C
P_t	Temperature dependence of phytoplankton growth rate (0.0663, Eppley [1972])	°C ⁻¹
B_t	Temperature dependence of heterotrophic respiration (0.08, Rivkin and Legendre [2001], López-Urrutia et al. [2006])	°C ⁻¹
Δef_{ml}	Differential for ef_{ml}	unitless
ΔN	Change in N	mmol m ⁻³
ΔI_0	Change in I_0	Einstein m ⁻² d ⁻¹
ΔT	Change in T	°C
$\Delta[Chl]$	Change in [Chl]	mmol m ⁻³
ΔMLD	Change in MLD	m

Table 2. Export ratios at different depths of integration, see Table 1 for acronyms.

Depth of integration		Equation
Euphotic depth (Z_{eu})		$ef_{eu} = \frac{NCP(0,Z_{eu})}{NPP(0,Z_{eu})} = 1 - \frac{1}{I_{eu}} \times \frac{1}{N_m} \times \frac{r_{HR}}{\mu_{max}}$ (9)
Fixed depth (Z_z)	$Z_z > Z_{eu}$	$ef_z = \frac{NCP(0,Z_{eu})}{NPP(0,Z_{eu})} \times e^{-\frac{Z_z - Z_{eu}}{Z^*}} = ef_{eu} \times e^{-\frac{Z_z - Z_{eu}}{Z^*}}$ (14)
	$Z_z < Z_{eu}$	$ef_z = \frac{NCP(0,Z_z)}{NPP(0,Z_z)} = 1 - \frac{1}{I_z} \times \frac{1}{N_m} \times \frac{r_{HR}}{\mu_{max}}$ (16a)
		$ef_z = \frac{NCP(0,Z_z)}{NPP(0,Z_z)} = 1 - \frac{I_{eu}}{I_z} (1 - ef_{eu})$ (16b)

Accepted Article

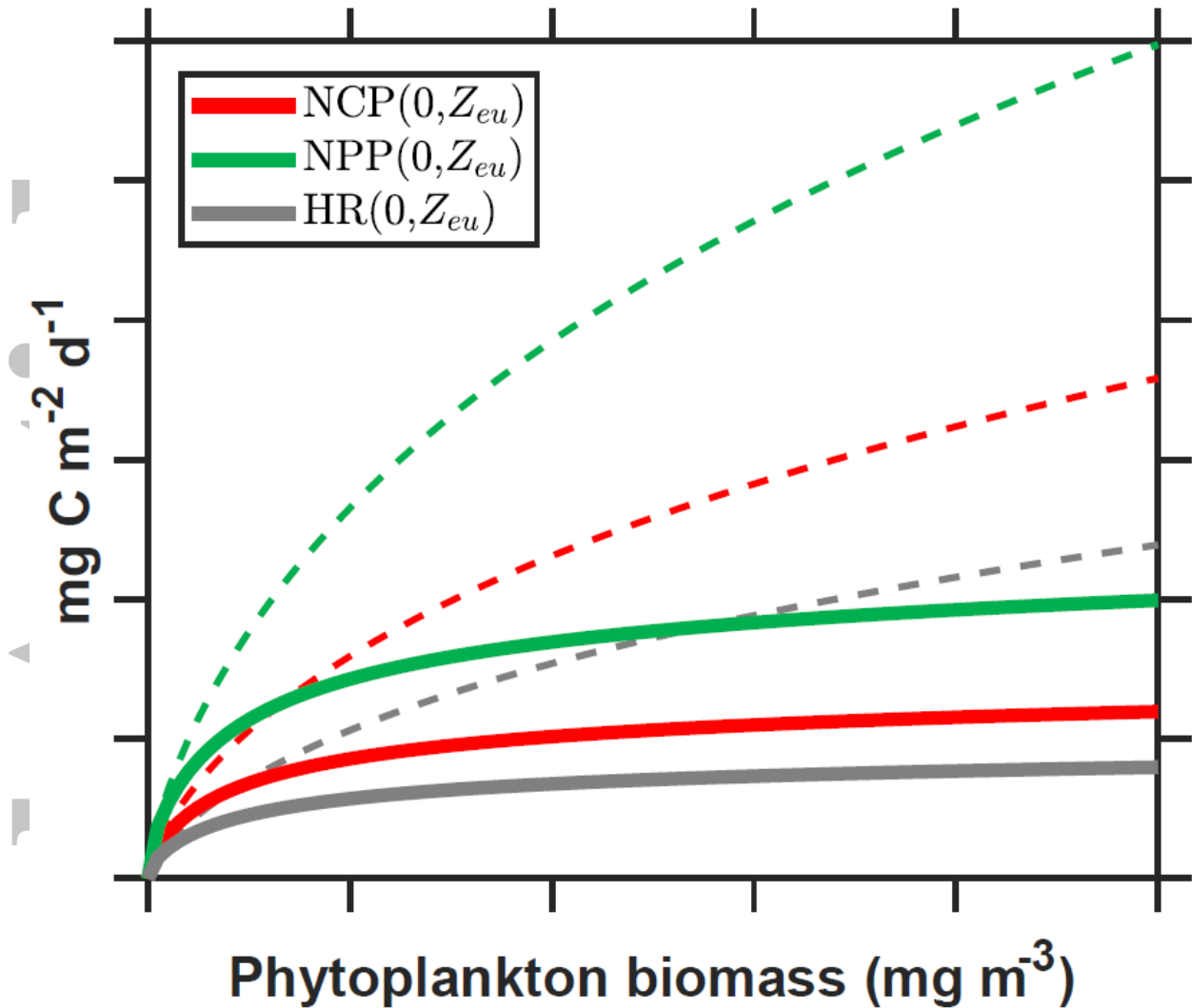


Figure 1. Schematic diagram of net community production (NCP), net primary production (NPP) and heterotrophic respiration (HR) integrated over the euphotic depth (Z_{eu}). Light attenuation coefficient (K_l) is a function of chlorophyll a concentration ($[Chl]$) [Morel *et al.*, 2007], which is in turn modeled as a function of phytoplankton biomass concentration (C) based on the autotrophic carbon to $[Chl]$ ratio ($C:[Chl]$). Dashed lines represent $\text{NCP}(0, Z_{eu})$, $\text{NPP}(0, Z_{eu})$, $\text{HR}(0, Z_{eu})$ derived using a constant $C:[Chl]$ of 90 [Arrigo *et al.*, 2008]. Solid lines represent $\text{NCP}(0, Z_{eu})$, $\text{NPP}(0, Z_{eu})$, $\text{HR}(0, Z_{eu})$ with variable $C:[Chl]$ estimated using the empirical relation between C and $[Chl]$ derived by Jakobsen and Markager [2016].

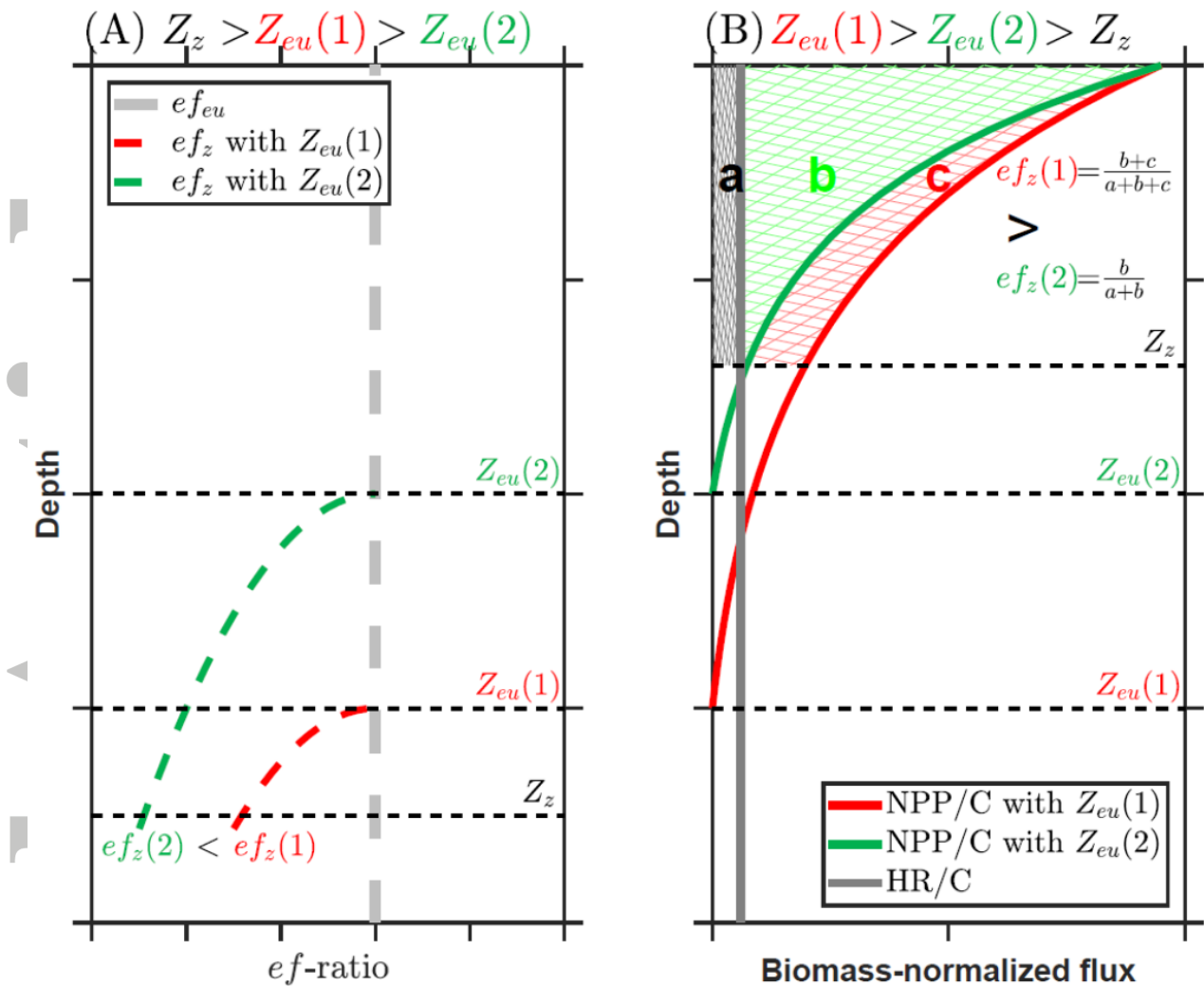


Figure 2. Schematic diagram of the export ratio as a function of the integration depth (i.e., depth horizon of measurement). (A) Case where the depth of integration Z_z is deeper than the euphotic depths and $Z_{eu}(1) > Z_{eu}(2)$. Particles are modeled to exponentially attenuate with depth (red and green dashed curves). Because $Z_{eu}(1) > Z_{eu}(2)$, the export production with $Z_{eu}(2)$ (green-dashed curve) has experienced more attenuation than the export production with $Z_{eu}(1)$ (red-dashed curve) at depth Z_z . (B) Case where $Z_{eu}(1) > Z_{eu}(2)$ and the euphotic depths are deeper than the depth of integration Z_z for net community production (NCP), net primary production (NPP), and heterotrophic respiration (HR). Gray line represents the biomass-normalized HR. Red and green lines represent biomass-normalized NPP with $Z_{eu}(1)$ and $Z_{eu}(2)$, respectively. $Z_{eu}(1) > Z_{eu}(2)$ implies that light attenuation for the red line is weaker than for the green line. The export ratios for $Z_{eu}(1)$ and $Z_{eu}(2)$ are $ef_z(1) = \frac{b+c}{a+b+c}$ and $ef_z(2) = \frac{b}{a+b}$, where a , b and c represent the areas of the hatched regions. Geometrically, $ef_z(1) = \frac{b+c}{a+b+c} > ef_z(2) = \frac{b}{a+b}$.

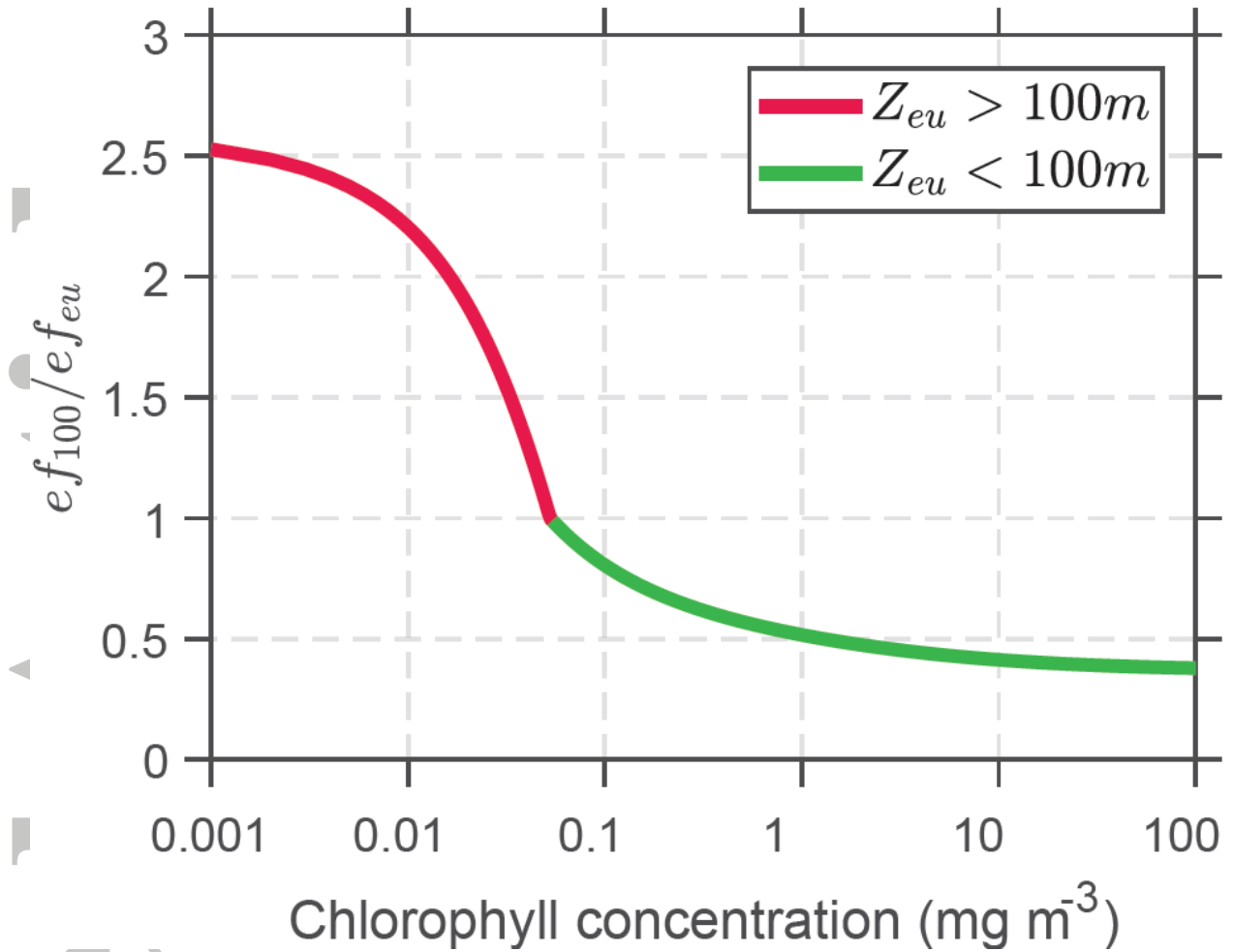


Figure 3. Export ratio at 100 m (ef_{100}) normalized to the export ratio at the euphotic depth (ef_{eu}) as a function of the chlorophyll a concentration. ef_{100} is calculated from equations 14 and 16. ef_{eu} is derived using equation (9). We select a remineralization length scale of $Z^* = 100$ m, a half-saturation constant for PAR of $k_m^I = 4.1$ Einstein $m^{-2} d^{-1}$, and a surface radiation beneath the water surface of $I_0 = 50$ Einstein $m^{-2} d^{-1}$. To calculate ef_{100}/ef_{eu} when the euphotic depth is deeper than 100 m, we set $ef_{eu} = 0.2$ which is in line with the typical value for the global ocean. Note that the abscissa is on a logarithmic scale.

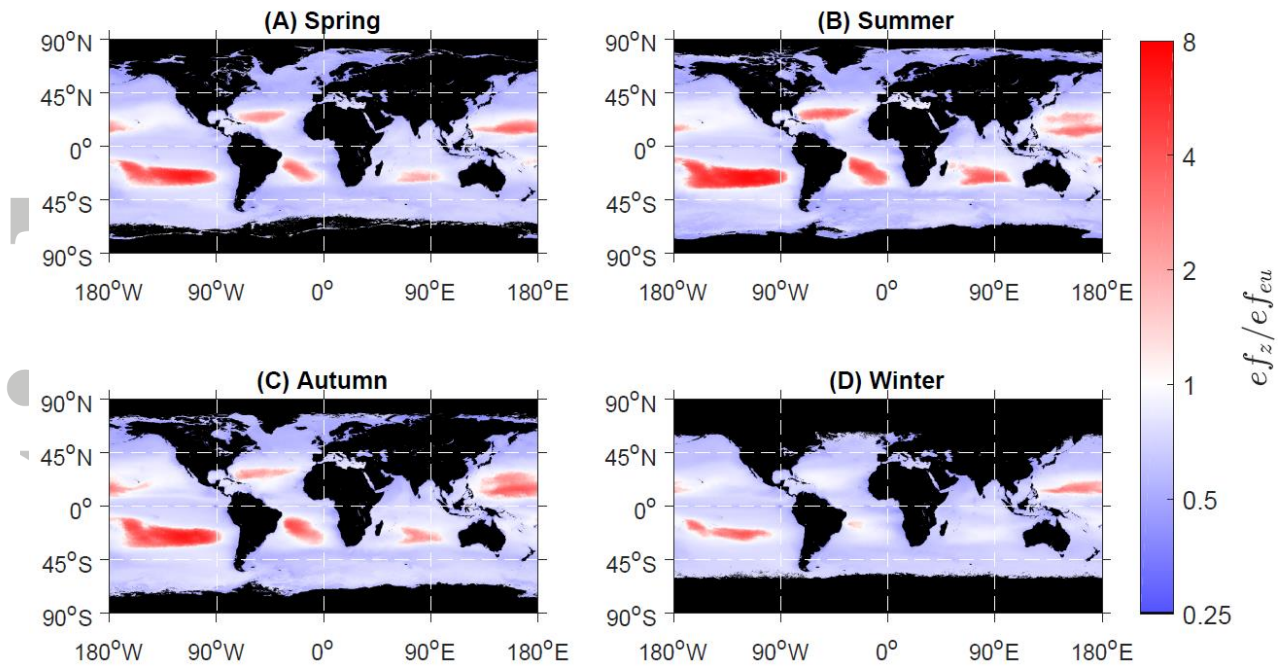


Figure 4. Global distribution of seasonally-averaged ef_{100}/ef_{eu} . ef_{100} is calculated from equations 14 and 16. ef_{eu} is derived using equation (9). In the Northern Hemisphere, seasons are defined as: spring (March–May), summer (June–August), autumn (September–November), and winter (December–February). In the Southern Hemisphere, seasons are defined as: spring (September–November), summer (December–February), autumn (March–May), and winter (June–August). Note that the ratio is shown on a logarithmic scale.

Accepted Article

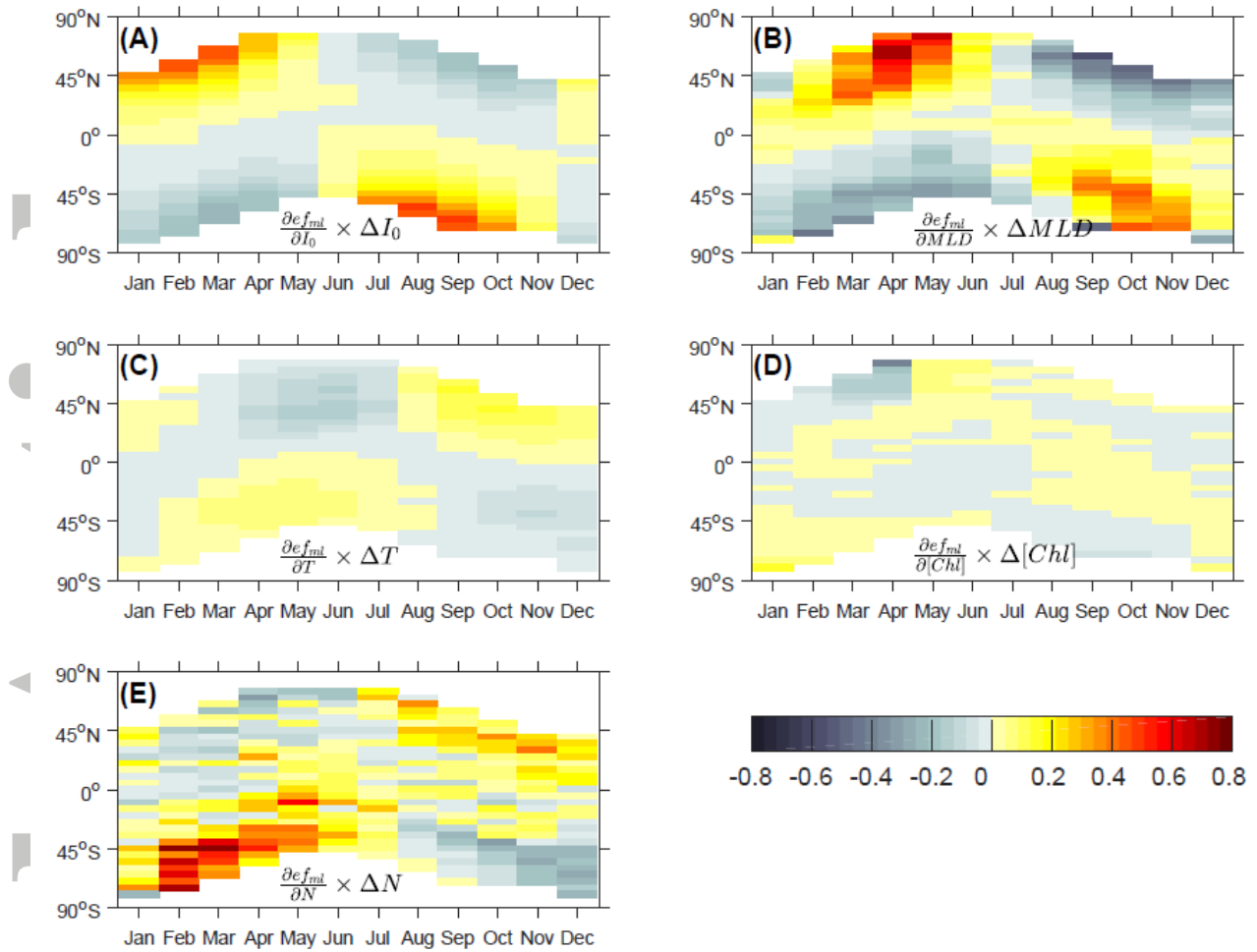


Figure 5. Hofmøller plots of the climatology of seasonal variations in the export ratio at the base of the mixed layer due to (A) photosynthetically active radiation just beneath water surface (I_0), (B) mixed layer depth (MLD), (C) sea surface temperature (T), (D) chlorophyll a concentration ($[Chl]$), and (E) nutrient concentration (N). Horizontal and vertical axes represent months and latitudes, respectively. Each row reflects a zonal average for each month. White areas represent missing values. Calculations are based on equation (24), noting that since $1 - e_{f_{ml}}$ is included in equations (19-23) describing all individual parameters, it is normalized in the derivation. See the supplementary material for the spatial distribution of each (A-E) contribution.